ARTICLE NO. 77-1271R

Noise Component Method for Airframe Noise

Martin R. Fink*
United Technologies Research Center, East Hartford, Conn.

A method was developed for predicting aerodynamic noise radiated by an airframe. Separate contributions are calculated for the clean wing, horizontal tail, vertical tail, landing gear, leading-edge slats and flaps, and trailing-edge flaps. Each noise component is predicted using scaling laws appropriate to that component, with amplitudes matched to available data. Spectra calculated by this method, the NASA Aircraft Noise Prediction Program (ANOPP) total aircraft method, and the drag element method are compared with flyover noise data for a twin-propeller lightplane, a business jet, and a jumbo jet.

Nomenclature

b = wing, horizontal tail, or vertical tail span
c_F = total chord of trailing-edge flaps
D = wheel tire diameter
f = ⅓ octave center frequency
f_{max} = frequency for maximum amplitude of ⅓ octave spectrum
h = altitude
N = number of wheels per landing-gear assembly
p^2 = mean square acoustic pressure
r = far field distance to observer
S = wing, horizontal tail, or vertical tail gross area
S_F = gross area of wing trailing-edge flaps
V = flight velocity
Y = sideline distance
α = rms turbulence level
δ = wing, horizontal tail, or vertical tail trailing-edge turbulent boundary-layer thickness
δ_F = deflection angle of trailing-edge flaps
Λ_{TE} = sweepback angle of trailing edge
ν = kinematic viscosity
ϕ = sideline angle
θ = polar angle

Introduction

NOISE emission from current airplanes is dominated by propulsion-system noise. Certification levels for aircraft noise, as specified in 1969 under Federal Air Regulation (FAR) 36, have been achieved by use of either high-bypass ratio turbofan engines and a relatively small amount of duct lining, or low bypass ratio turbofan engines plus noise-attenuating nacelles. Lower levels of propulsion-system noise have been achieved with high-bypass ratio turbofan engines combined with extensive inlet and discharge duct acoustic suppression. These reductions of propulsion-system noise do not cause equal reductions of total aircraft noise at the approach certification point. Airframe noise, generated by motion of aircraft external surfaces through the air, is believed to be only about 5-10 dB below the 1977 revision to FAR 36.[1] Airframe noise at approach may impose a fundamental noise floor roughly equal to the demonstrated noise from high bypass ratio turbofans with extensive inlet and exhaust acoustic suppression, at approach power setting. Future certification levels must be based on what can be achieved with economically viable airframes and propulsion systems. Thus it is necessary to understand the fundamental processes of airframe noise radiation.

Several methods for predicting airframe noise were examined by NASA as part of the Aircraft Noise Prediction Program (ANOPP). Two airframe noise prediction methods, the total aircraft method for aircraft in the clean configuration, and the drag element method for all configurations, were recommended[2] and were subsequently programmed by NASA Aircraft Noise Prediction Office. Verification by comparisons with measured airframe noise spectra have not been published for the total aircraft method and were available for only a few cases for the drag element method.

More recently, a noise component method was developed for the Federal Aviation Administration under Contract DOT-FA76WA-3821.[3] The purposes of this paper are to describe that method, including recent revisions, and to evaluate the validity of these several airframe noise prediction methods by comparisons between calculated and measured flyover noise spectra.

NASA ANOPP Methods

Two NASA ANOPP methods for calculating airframe noise were obtained from NASA within one computer program. Option 1 of that computer program is the total aircraft noise method developed by Hardin[2] for clean airframes. It was derived from a regression analysis of measured peak OASPL for selected aircraft flyovers. These OASPL's were actual measured values, uncorrected for irregularities in the spectra. Mean square acoustic pressure was assumed to vary inversely with distance squared. Exponents for velocity, wing area, wing aspect ratio, and gross weight were determined, which minimized the rms error. The data base did not include any jet aircraft other than the C-5A. Comparisons between measured and calculated spectra for this method had not been published.

Options 2 through 8 of the NASA-supplied computer program calculate airframe noise from seven components as given by Revell's drag element method.[4] These components are the noise caused by wing profile drag (including trailing edge flaps), wing induced drag, and profile drag of the fuselage, nacelles, horizontal tail, landing gear, and leading-edge slat. Input data include flight speed, altitude, airframe geometry, lift coefficient, and the drag coefficient for each component. Flow velocity at the wing upper surface trailing edge, as calculated from the magnitude and chordwise location of wing maximum velocity,[4] also is needed. Considerable aerodynamic information, therefore, is required for calculation of airframe noise by this method.

Presented as Paper 77-1271 at the AIAA 4th Aeroacoustics Conference, Atlanta, Ga., Oct. 3-5, 1977; submitted Dec. 28, 1977; revision received April 26, 1979.

Index categories: Aeroacoustics, Noise.

*Senior Consulting Engineer, Aerodynamics. Associate Fellow AIAA.

FAA Noise Component Method

The new method described herein is an airframe noise component method. That is, noise radiation from each individual portion of the airframe is calculated without regard for other noise sources. Each noise component is assumed to be given by whatever aeroacoustic mechanism, velocity dependence, directivity, and spectrum seems to be appropriate. In contrast, the drag element method had attributed all components of airframe noise to essentially the same mechanism so that all had the same functional dependence and normalized spectrum shape.

The individual noise-radiating airframe components represented by the method developed herein are sketched in Fig. 1. Noise is produced by the clean wing, horizontal tail, and vertical tail. Noise contributions from the nose landing gear and main landing gear are calculated separately because each generally has a different size and therefore a different peak frequency. Noise from the trailing-edge flaps is calculated independently of whether the landing gear is extended or retracted. Noise from leading-edge slats and flaps also is included.

Clean Wing and Tail Surfaces

Noise radiation from clean wing and tail surfaces is assumed to be caused by convection of turbulent boundary layers past the trailing edges of those surfaces.[5] The resulting trailing-edge noise radiation is well understood analytically.[6] Far-field acoustic pressure should have the functional dependence

$$\overline{p^2} \sim \alpha^2 (\delta b/r^2) V^5 \cos^2\Lambda_{TE} \cos^2\phi \cos^2(\theta/2) \qquad (1)$$

This directivity function, uncorrected for convective amplification, was shown in Fig. 18 of Ref. 7 to give reasonable prediction of flyover data. Apparent absence of convective amplification may mean that relative velocity between the turbulent eddies and the observer, rather than between the trailing edge and the observer, determines the radiation pattern. A comparison with data for a number of DC-10 flights, taken from Fig. 14 of Ref. 8, is given in Fig. 2. To evaluate the validity of this scaling law, boundary-layer thickness δ was calculated as that for a flat-plate turbulent boundary layer at the trailing edge of the mean geometric chord S/b.

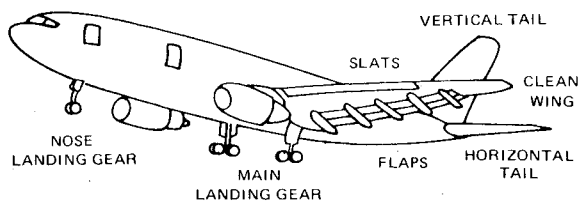

Fig. 1 Individual noise-radiating components.

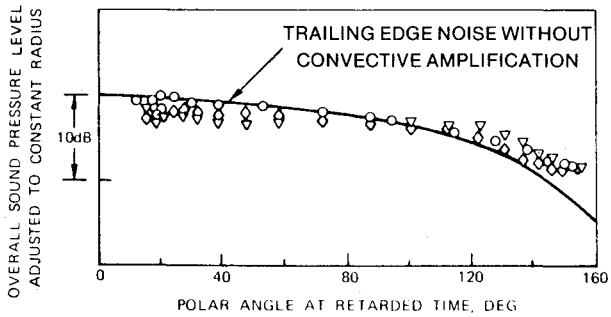

Fig. 2 Comparison of several measurements of DC-10 airframe noise directivity at constant radius with calculated trailing edge noise directivity.

$$\delta = 0.37(S/b)(VS/b\nu)^{-0.2} \qquad (2)$$

Trailing-edge sweepback angle Λ_{TE} was assumed equal to zero. Maximum mean square acoustic pressure should then be proportional to the product of boundary-layer thickness δ and wing span b, divided by altitude squared, for all wing planforms.

This prediction is checked in Fig. 3, which is a plot of measured maximum flyover noise for clean airframes adjusted for boundary-layer thickness as OASPL $-$ 10 log $(\delta b/h^2)$, versus velocity. The data from Table 2 of Ref. 9 are levels for the idealized (smoothed) spectra rather than the composite (actual) spectra. Open symbols represent measurements from microphones mounted on posts and are therefore approximately 3 dB above free field, as with FAR 36 certification tests. Solid symbols are data from flush-mounted microphones (6 dB above free field as published) decreased 3 dB to allow direct comparison. All airframe noise predictions are assumed to apply to FAR 36 data, 3 dB above free field.

Adjusted OASPL for the aerodynamically clean high-performance sailplanes, F-106B supersonic delta-wing interceptor, and BAC 1-11 jet transport are closely matched by

$$\text{OASPL} = 50 \log(V/100\text{kt}) + 10 \log(\delta b/h^2) + 101.5 \text{ dB} \qquad (3)$$

which is the lower solid line in Fig. 3. Note that aspect ratio does not appear in this equation, although aspect ratio differs by an order of magnitude from the F-106B to the sailplanes. Data for conventional low-speed aircraft in the clean configuration were 8 dB higher (the upper solid line). Data for most jet aircraft were about 6 dB above the line for aerodynamically clean sailplanes, as shown by the dashed line. However, spectra for clean jet aircraft generally differed in shape from those of the other aircraft. As discussed later,

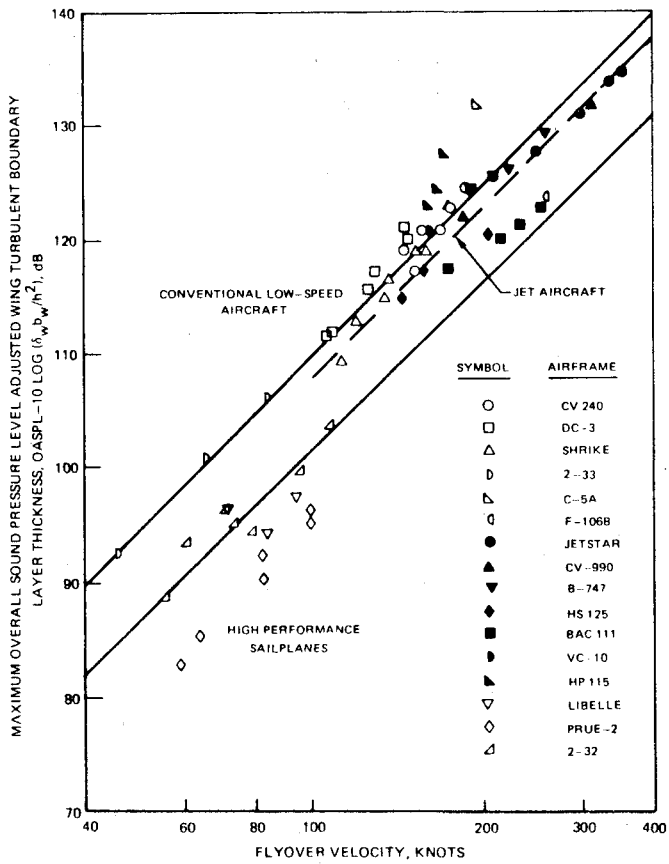

Fig. 3 Maximum overall sound pressure level for clean airframes, normalized with respect to product of wing span and wing boundary layer thickness.

an additional noise mechanism occurs. Trailing-edge noise for jet aircraft should be calculated using the constant appropriate for aerodynamically clean aircraft.

When spectra for wings and horizontal tail surfaces were calculated, it was found that total spectrum was best predicted if the constant was 2 dB below these numbers. Then OASPL for an aerodynamically clean wing or horizontal tail is given by

$$\text{OASPL} = 50 \log(V/100\text{kt}) + 10 \log(\delta b/h^2) \times \cos^2\phi \cos^2(\theta/2) + 101.3\text{dB} \quad (4)$$

Noise from a vertical tail is given by this equation with $\cos^2\phi$ replaced by $\sin^2\phi$. Maximum amplitude is predicted to occur at about 71 deg from the approach direction, before the airplane reaches the overhead position.

If the major noise generation mechanism for airframe noise of aerodynamically clean airframes is trailing edge noise, the spectrum shape for airframe noise should be given by the existing solutions for trailing-edge noise. A semi-empirical equation for normalized spectral density of trailing-edge noise from externally blown flaps was given as Eq. (12) of Ref. 10. Converting to third octave sound pressure level ($\text{SPL}_{1/3}$) relative to overall sound pressure level OASPL, and center frequency f relative to the center frequency $f_{\max}$ which yields maximum $\text{SPL}_{1/3}$,

$$\text{SPL} - \text{OASPL} = 10 \log 0.613 (f/f_{\max})^4 [(f/f_{\max})^{3/2} + 0.5]^{-4} \quad (5)$$

The spectrum shape given by this equation is compared in Fig. 4 with the nondimensional airframe noise spectrum recommended for use with the NASA ANOPP total aircraft analysis (Fig. 4 of Ref. 2). The two dotted curves are boundaries of smoothed nondimensional spectra from 28 flights of five different airplanes tested by Healy.[9] The solid curve drawn between these boundaries is used in the total aircraft method.[2] The open symbols calculated from Eq. (5) are within ± 1 dB of the solid data-average curve for frequency ratios up to 8. At larger frequency ratios they decay less rapidly than the data. The measured rapid spectrum decay at large frequency ratios was caused by atmospheric attenuation of the radiated flyover noise. This behavior had been approximated by Revell[4] as an exponential decay of mean square acoustic pressure. Following that guide, a correction term

$$\Delta\text{SPL} = -0.03(r/500\text{ft}) |(f/f_{\max}) - 1|^{3/2} \quad (6)$$

was added to Eq. (5). Here, $f_{\max}$ is always taken as the frequency for maximum wing trailing-edge noise. Resulting normalized amplitudes, shown in Fig. 4 as solid symbols, closely match the measured spectrum decay at large frequency ratios. Strouhal number at maximum amplitude was arbitrarily taken as

$$f_{\max}\delta/V = 0.1 \quad (7)$$

This nondimensional spectrum should be valid only for an untapered wing. Strip-theory calculations were conducted for a range of taper ratios (tip chord divided by root chord). It was found that decreasing the taper ratio to 0.25 caused less than 1.2 dB change in 1/3 octave levels. However, wings with zero tip chord were predicted to have higher normalized amplitude at large frequency ratios. For highly tapered wings as with a supersonic transport,

$$\text{SPL} - \text{OASPL} = 10 \log \times \{0.485(f/f_{\max})^4 [0.5 + (f/f_{\max})^{1.35}]^{-4}\} \quad (8)$$

should be used instead of Eq. (5). All spectra shown herein were calculated from Eqs. (5-7). Effects of lift coefficient are neglected.

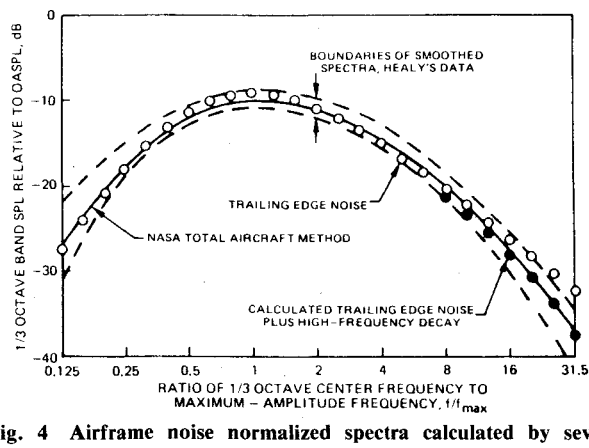

Fig. 4 Airframe noise normalized spectra calculated by several methods.

Spectra calculated from Eqs. (5) and (7) recently have been found to agree with trailing-edge noise measurements for a 9-in. chord NACA 0018 airfoil at zero incidence.[11] At the test airspeeds from 200-400 ft/s, these spectra were below tunnel background noise but were extracted by use of a directional microphone and were shown to originate at the trailing edge.

Spectra measured with jet aircraft generally include a moderate-frequency broadband peak which does not change frequency as flight speed is varied. This peak occurs in a frequency range of strong propulsive-system noise from the idling turbojet or turbofan engines. Engine noise should not vary with sideline angle while airframe trailing edge noise should vary with cosine squared of the angle from the flyover plane. (Calculated vertical tail noise is low enough to be neglected for this comparison.) These variations may explain the sideline directivity results shown by NASA in Fig. 9 of Ref. 12 for the Lockheed JetStar and by RAE in Fig. 24 of Ref. 13 for the Vickers VC 10. From both sets of OASPL data, it was concluded that sideline noise of a clean airframe varied only inversely with radius squared, without an additional dependence on sideline angle. Unpublished NASA sideline noise measurements for the Convair 990 in the clean configuration (run 3, 315 knots) were obtained for detailed examination. Measured spectra were examined at the retarded time for which the Doppler effect on frequency was closest to zero.

Resulting variations of overall sound pressure level, and 1/3 octave sound pressure levels at 200 and 1600 Hz center frequencies, with sideline distance, are plotted in Fig. 5. Also shown are variations that would be expected for acoustic radiation from a horizontal surface and for a variation inversely with radial distance but independent of sideline angle. Notice that for the lower frequency, where airframe noise should greatly exceed propulsive noise, the rapid decrease predicted for surface-radiated noise did occur. OASPL, and the higher-frequency noise attributed here to propulsive-system noise, matched the smaller predicted decay rate expected for an axisymmetric noise source.

Trailing Edge Flaps

The effect of trailing-edge flap deflection on noise amplitude can be illustrated by use of the measured spectra[13] for the Vickers VC 10 aircraft. Spectra had been obtained at constant airspeed for the clean airframe with flaps retracted and for 20, 35, and 45 deg flap deflection angles. Noise increments caused by flap deflection were determined by logarithmic subtraction of the flaps-retracted spectrum. The spectra of these three noise increments, plotted in Fig. 6a, all had approximately the same shape. Amplitude increased as

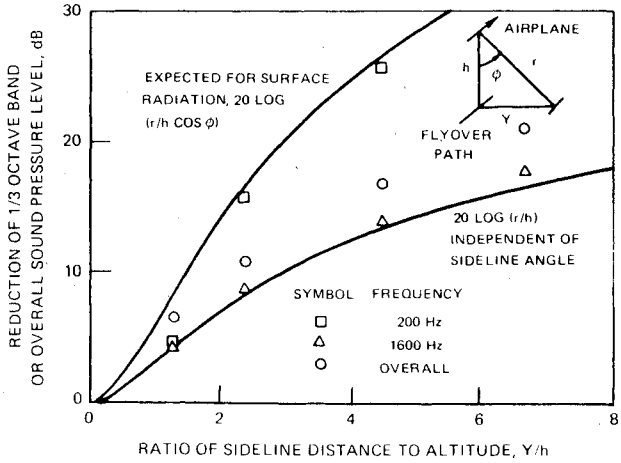

Fig. 5 Variation of overall and 1/3 octave sound pressure levels with sideline distance for Convair 990, evaluated at constant retarded time.

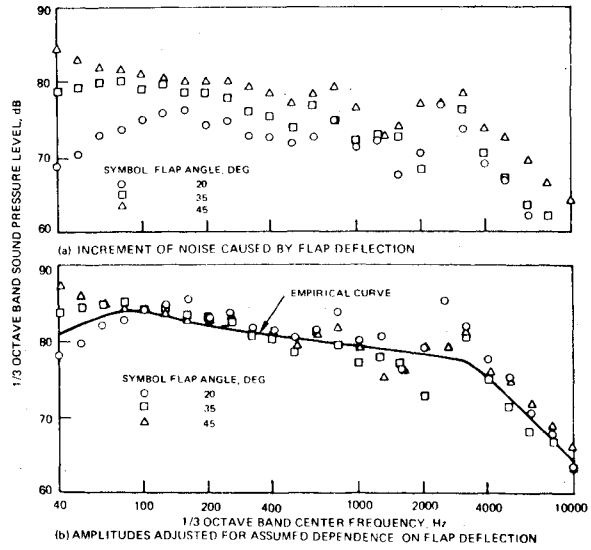

Fig. 6 Dependence of trailing edge flap noise on sine squared of deflection angle for Vickers VC 10.

flap deflection was increased. By arbitrarily assuming that trailing-edge flap SPL varies with sine squared of the flap deflection angle, the three spectra were coalesced (Fig. 6b).

The increase of flyover noise caused by deflection of trailing-edge flaps was assumed to vary directly with flap area, inversely with far field distance squared, and directly with airspeed to the sixth power. Frequency was scaled as a Strouhal number relative to flap total chord (flap total area divided by flap span). Using these and the empirical dependence on sine squared of deflection angle, normalized spectra for measured noise from trailing-edge flaps were obtained. These are plotted in Fig. 7. (Values shown were measured with flush microphones and are 6 dB above free field.)

Spectra for the Vickers VC 10 and Boeing 747, and also for the Douglas DC-10[7] (not shown) remain large at Strouhal numbers up to 60, while spectra for less complicated trailing-edge flap systems decay rapidly above a Strouhal number of 20. Judged from unpublished flyover data, the directivity of trailing-edge flap noise appears to be that of a lift dipole normal to the flight direction, corrected for convective amplification.

Landing Gear

Noise from extended landing gear was calculated from empirical equations fitted to data[14] for two-wheel and four-wheel models. Single-wheel landing gear were assumed to be 3 dB quieter than two-wheel gear having the same wheel diameter D. For frequencies of high annoyance, the directivity pattern can be taken as independent of sideline angle. With N wheels, where N is 1 or 2, the 1/3 octave spectrum of one landing-gear assembly was taken as

$$\mathrm{SPL} = 60\log(V/194\mathrm{kt}) + 20\log(D/r) + 130 + 10\log 4.5 \times N(fD/V)^2[12.5 + (fD/V)^2]^{-2.25} \quad (9)$$

Measured spectra for four-wheel models were found to underestimate full-scale landing-gear noise at high frequencies. Data for the Vickers VC 10 and Boeing 747 landing gear were better predicted by

$$\mathrm{SPL} = 60\log(V/194\mathrm{kt}) + 20\log(D/r) + 123 + 10\log 0.3(fD/V)^2[1 + 0.25(fD/V)^2]^{-1.5} \quad (10)$$

per gear assembly, which has a less rapid high-frequency decay rate. Directivity is that of a monopole with convective amplification.

Leading Edge High-Lift Devices

Deflection of leading-edge flaps was assumed to increase the wing boundary-layer turbulence intensity to that for conventional subsonic aircraft, 8 dB above the level given by Eq. (4). Leading-edge slats were assumed to increase the wing noise to 11 dB above Eq. (4) and also to generate noise caused by turbulent boundary-layer flow past their own trailing edges at high local velocity. This noise was assumed to have the same amplitude as the increased wing noise, with peak

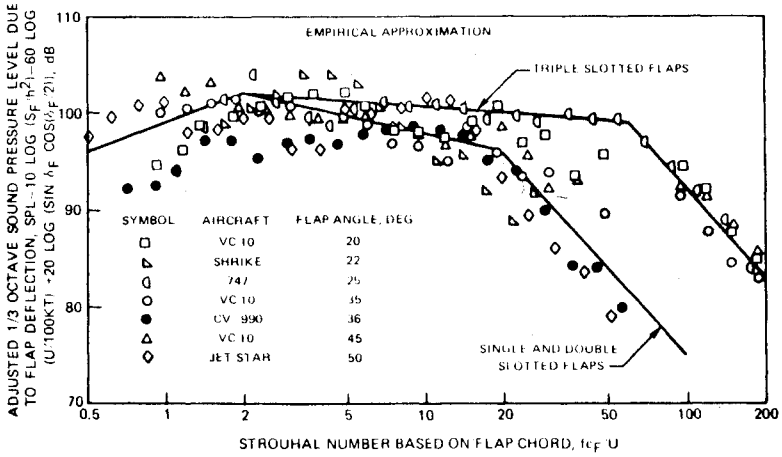

Fig. 7 Normalized spectra of measured trailing edge flap noise.

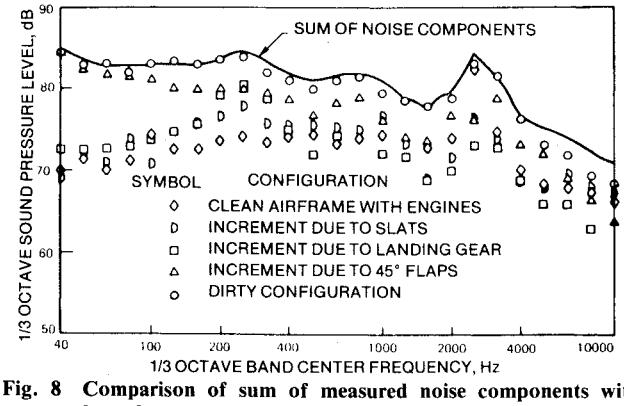

Fig. 8 Comparison of sum of measured noise components with measured total noise for Vickers VC 10 aircraft in approach configuration.

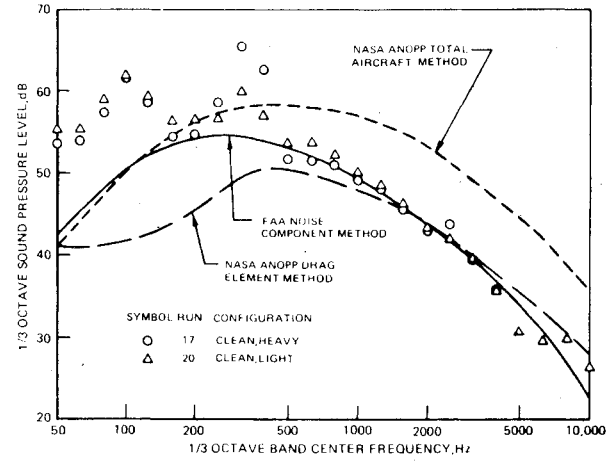

Fig. 9 Measured and calculated flyover noise spectra for Aero Commander Shrike in clean configuration at 113 knots airspeed.

frequency calculated from Eqs. (7) and (2) for the slat chord. The resulting calculated noise spectrum caused by slat extension generally matches the noise increment caused by slat extension on the Vickers VC 10 airplane.[13]

Summation of Noise Components

The calculated components are summed as noninteracting uncorrelated noises. Validity of this approach can be checked by comparing measured flyover noise spectra, at constant airspeed, for an airframe with components extended individually and in combination. Flights of this type had been conducted for the Vickers VC 10 at 600 ft altitude and approximately 160 knots airspeed.[13] The spectrum measured for the clean airframe with idling engines was logarithmically subtracted from those for the airframe with only the leading-edge slats extended, only the landing gear extended and wheel well doors closed, and only the trailing-edge flaps at 45 deg deflection. Resulting noise increments from each of these components are plotted in Fig. 8. Also plotted as a solid line is the logarithmic sum of measured noise for the clean airframe, including engines, and those three noise increments. This experimental prediction of total airframe noise in the approach configuration is seen to be in excellent agreement with the measured spectrum up to 4000 Hz center frequency. For at least this one aircraft, the noise components at approach either do not interact or have compensating interactions.

Comparisons with Flyover Data

Aero Commander Shrike

Measured spectra[9] for the Aero Commander at 113 knots in the clean configuration and two gross weights are plotted in Fig. 9. Peak amplitudes in the spectra occurred as a possible ground reflection near 100 Hz and noise from the feathered propellers in the 315 and 400 Hz 1/3 octave bands. The spectrum calculated by the total aircraft method has an OASPL which matches that of the actual data including those peaks. This method overestimates the measured 1/3 octave SPL's by about 5 dB at frequencies above 500 Hz. Spectra calculated by both the drag element method and the noise component method are in good agreement with data and with each other at frequencies above the feathered-propeller noise peak.

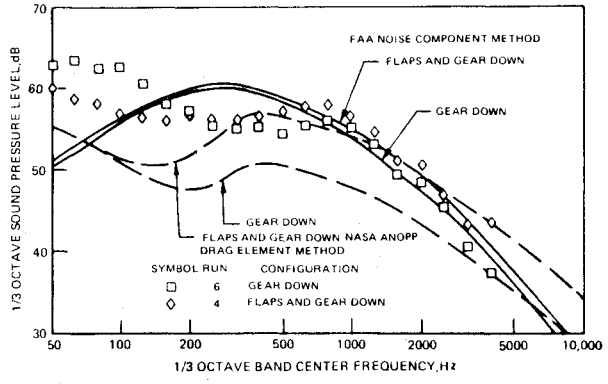

Fig. 10 Measured and calculated flyover noise spectra for Aero Commander Shrike with landing gear extended, and with landing gear and trailing edge flaps extended, at 113 knots airspeed.

NASA spectra[15] for this airspeed and two flights, one with the landing gear extended and one with landing gear and single-slotted trailing-edge flaps extended, are shown in Fig. 10. These data had been measured with flush-mounted microphones and are plotted 3 dB lower than the measured levels, for direct comparison with the predictions and clean-configuration data. Extending the flaps decreased the low-frequency noise from the landing gear cavity but increased the noise several dB at greater than 200-Hz center frequency. Thus OASPL was decreased but PNL was increased by flap extension with the landing gear down. Landing-gear noise is calculated by the drag element method to peak at a relatively low frequency, as with the C-5A airplane, and to become unimportant above 400 Hz. Measured noise with landing gear down was underpredicted by the drag element method and was closely predicted by the noise component method. Noise measured with both the gear and flaps down, at frequencies above 500 Hz, was closely predicted by both methods. Data for this configuration did not extend high enough in frequency to check the difference between predictions above 5000 Hz. For the frequency range of good agreement, noise from the trailing-edge flaps as predicted by the drag element method is in good agreement with the sum of measured flap and landing gear noise.

Lockheed JetStar

Flyover noise data for this aircraft and for the Boeing 747 were obtained by NASA[12,15] with flush-mounted microphones, and these data have been decreased 3 dB for this comparison. A spectrum at 182 knots with landing gear down is plotted in Fig. 11. As with the comparison for the Aero Commander Shrike, landing-gear noise as calculated by the drag element method was predicted to occur only at low frequencies. This method underestimated the measured noise by about 10 dB between 1000 and 2500 Hz and about 5 dB over most other frequencies. The noise component method gave the general level of the data, which oscillated roughly ±5 dB relative to this prediction. Worst agreement occurred near the high-frequency peak.

Measured spectra are shown in Fig. 12 for the JetStar at 170 knots with trailing-edge flaps down and at 158 knots with

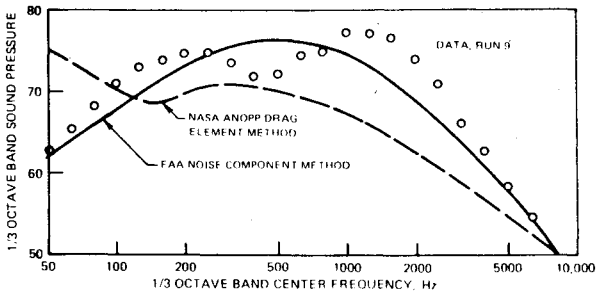

Fig. 11 Measured and calculated flyover noise spectra for Lockheed JetStar with landing gear extended at 182 knots airspeed.

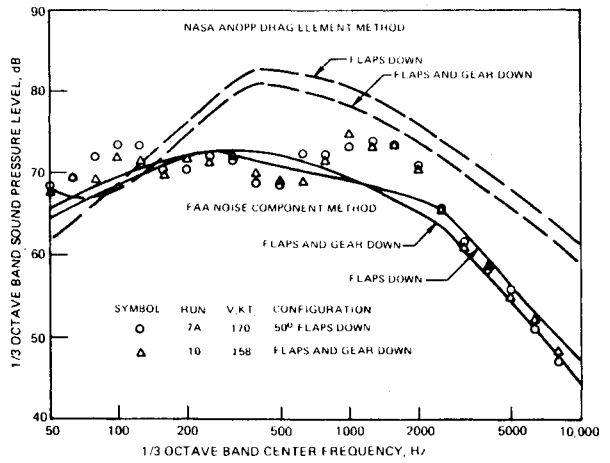

Fig. 12 Measured and calculated flyover noise spectra for Lockheed JetStar with trailing edge flaps extended at 170 knots and with flaps and landing gear extended at 158 knots.

landing gear and flaps down. There was no systematic difference between the two measured spectra; the decrease of flap noise caused by reduced velocity was approximately matched by the added landing-gear noise. The drag element method predicts a large amount of trailing-edge flap noise caused by the large value of profile drag coefficient at 50 deg flap deflection. Airframe noise generally is overestimated about 10 dB for this configuration. Decreasing the airspeed and lowering the landing gear is predicted to cause about 2 dB noise reduction, contrary to the lack of change in measured levels. In contrast, the noise component method generally predicts these spectra except for the broad peak between 1000 and 2000 Hz frequencies. Spectra calculated by that method for the two configurations and airspeeds intersect each other, in agreement with the data.

Spectra measured at NASA with the clean Boeing 747, Convair 990, and Lockheed JetStar[12,15] jet aircraft had their OASPL and perceived noise level dominated by this peak near 1600 Hz center frequency. In contrast, spectra for the Aero Commander Shrike as measured with the same test equipment[15] had only a single lower-frequency peak. Major peculiarities of the jet aircraft peak are that its center frequency does not vary significantly with flight speed or aircraft type, and its variation of amplitude with sideline angle is only an inverse distance squared dependence without the dipole factor (cosine squared of angle from the flyover plane). The observed sideline dependence has been termed "monopole"[13] but a more appropriate word is "axisymmetric." Amplitude of this peak has been shown to vary approximately with flight speed to the fifth power and wing area to the first power.[16] Peak frequency was noted to match the flight-idle fan rotor blade passing frequency for both the Boeing 747 and Convair 990,[3] although the peak is broader and stronger than measured engine noise with these aircraft on the ground. This spectrum peak was therefore taken as

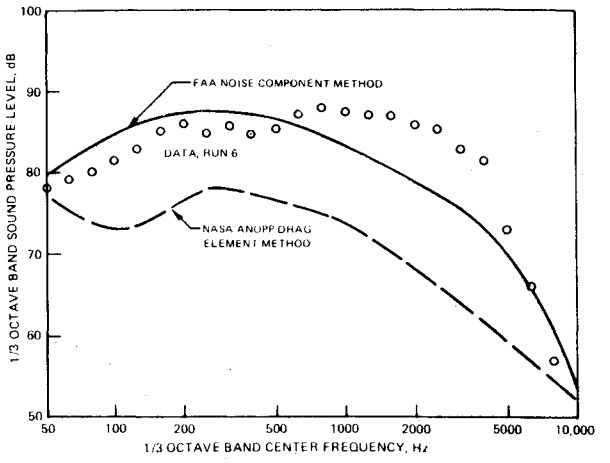

Fig. 13 Measured and calculated flyover noise spectra for Boeing 747 with landing gear extended at 222 knots airspeed.

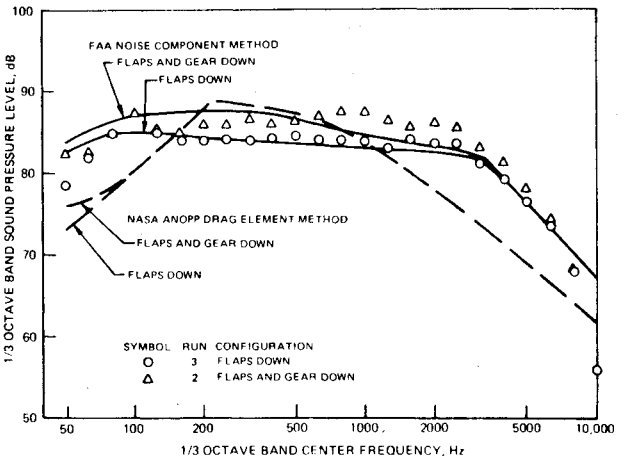

Fig. 14 Measured and calculated flyover noise spectra for Boeing 747 with trailing edge flaps extended, and with flaps and landing gear extended, at 204 knots airspeed.

propulsion-system noise caused by local separated flow within the inlet duct at low engine weight flow in forward flight.[3]

Boeing 747

A spectrum measured for the Boeing 747[12] at 233 knots with landing gear extended is plotted in Fig. 13. This aircraft has four four-wheel main landing gear and a two-wheel nose landing gear. As with other aircraft, the spectrum predicted by the drag element method for the airplane with gear extended matches that predicted for the clean airframe except at low frequencies. Measured 1/3 octave SPL's are underestimated by about 10 dB between 100 and 500 Hz frequencies and more than 15 dB in the peak centered at fan blade passing frequency. The noise component method is 2 to 3 dB high below 500 Hz, about 8 dB low for most of the higher-frequency peak, and in general agreement above 4000 Hz.

Spectra measured with the Boeing 747 at approximately 198 knots with trailing-edge flaps extended, and with flaps and landing gear extended, are plotted in Fig. 14. Extending the landing gear added 3-4 dB at frequencies from about 250-5000 Hz. Spectra predicted by the drag element method for the configuration with deflected flaps are about 5 dB too high between 200 and 500 Hz and about 8 dB too low between 2000 and 6300 Hz center frequencies. The increased noise caused by landing gear extension at high-annoyance frequencies was not predicted. The noise component method closely predicts the flaps-down spectrum because it is based in part upon this

spectrum. Also, it approximately predicts the spectrum measured with flaps and gear down. Differences of about 3 dB between predictions and data for the aircraft with flaps and gear extended may represent component interaction effects. These interactions have been measured with a Boeing 747 model to be of this general size.[17] The noise component method closely approximates the general spectrum shape. For aircraft with deflected trailing-edge flaps, the drag element method gives a spectrum which is too sharply peaked because it has the normalized shape associated with clean-airframe noise.

Conclusions

1) The noise component method correctly predicts amplitudes and spectrum shapes of measured flyover noise due to extended landing gear and trailing-edge flaps.

2) The drag element method correctly predicts the general level but not the spectrum shape of trailing-edge flap noise at moderate deflections. It poorly predicts noise from extended landing gear. Generally it correctly predicts clean-airframe noise.

Acknowledgment

This research was sponsored by the Department of Transportation, Federal Aviation Administration, under contract DOT-FA76WA-3821.

References

[1] Morgan, H. G. and Hardin, J. C., "Airframe Noise—The Next Aircraft Noise Barrier" *Journal of Aircraft*, Vol. 12, July 1975, pp 622-624.

[2] Hardin, J. C., Fratello, D. J., Hayden, R. E., Kadman, Y., and Africk, S., "Prediction of Airframe Noise," NASA TN D-7821, Feb. 1975.

[3] Fink, M. R., "Airframe Noise Prediction Method" FAA RD-77-29, March 1977.

[4] Revell, J. D., Healy, G. J., and Gibson, J. S., "Methods for the Prediction of Airframe Aerodynamic Noise," *Progress in Astronautics and Aeronautics: Aeroacoustics: Acoustic Wave Propagation; Aircraft Noise Prediction; Aeroacoustic Instrumentation;* Vol. 46, AIAA, N.Y. 1976, pp. 139-154.

[5] Fink, M. R., "Approximate Predictions of Airframe Noise," *Journal of Aircraft,* Vol. 13, Nov. 1976, pp 833-834.

[6] Ffowcs Williams, J. and Hall, L. H., "Aerodynamic Sound Generation by Turbulent Flow in the Vicinity of a Scattering Half Plane" *Journal of Fluid Mechanics,* Vol. 40, March 1970, pp 657-670.

[7] Munson, A. J., "A Modeling Approach to Nonpropulsive Noise," AIAA Paper 76-525, Palo Alto, Calif., July 1976.

[8] Pendley, R. E., "Recent Advances in the Technology of Aircraft Noise Control" *Journal of Aircraft*, Vol. 13, July 1976, pp 513-519.

[9] Healy, G. J., "Measurement and Analysis of Aircraft Far-Field Aerodynamic Noise" NASA CR-2377, Dec. 1974.

[10] Fink, M. R., "Prediction of Externally Blown Flap Noise and Turbomachinery Strut Noise," NASA CR-134883, Aug. 1975.

[11] Schlinker, R. H., "Airfoil Trailing Edge Noise Measurements with a Directional Microphone System" AIAA Paper 77-1269, Atlanta, Ga., Oct. 1977.

[12] Putnam, T. W., Lasagna, P. L., and White, K. C., "Measurements and Analyses of Aircraft Airframe Noise", *Progress in Astronautics and Aeronautics: Aeroacoustics: STOL Noise; Airframe and Airfoil Noise;* Vol. 45, AIAA, N.Y., 1976, pp. 363-378.

[13] Fethney, P., "An Experimental Study of Airframe Self-Noise," *Progress in Astronautics and Aeronautics: Aeroacoustics: STOL Noise; Airframe and Airfoil Noise;* Vol. 45, AIAA, N.Y., 1976, pp. 379-404.

[14] Heller, H. H. and Dobrzynski, W. M., "Sound Radiation From Aircraft Wheel-Well/Landing Gear Configurations." *Journal of Aircraft*, Aug. 1977, pp. 768-774.

[15] Lasagna, P. L. and Putnam, T. W., "Preliminary Measurements of Aircraft Aerodynamic Noise," AIAA Paper 74-572, Palo Alto, Calif., June 1974.

[16] Hersh, A. S., Putnam, T. W., Lasagna, P. L., and Burcham, F. W., Jr., "Semi-Empirical Airframe Noise Prediction Model and Evaluation With Flight Data" NASA TM X-56041, Dec. 1976.

[17] Shearin, J. G. and Fratello, D. J., "Airframe Noise of Component Interactions on a Large Transport Model" AIAA Paper 77-57, Los Angeles, Calif., Jan. 1977.